Simulating the EOR with self-consistent growth of galaxies

Master's thesis presentation

ETH Zürich, University of Zürich

Simulating the Epoch of Reionization

- The 21-cm signal
- Expression the 21-cm signal [1], [2]
- The current state of simulations

The 21-cm signal

The *brigthtness temperature* describes the intensity of the 21-cm line

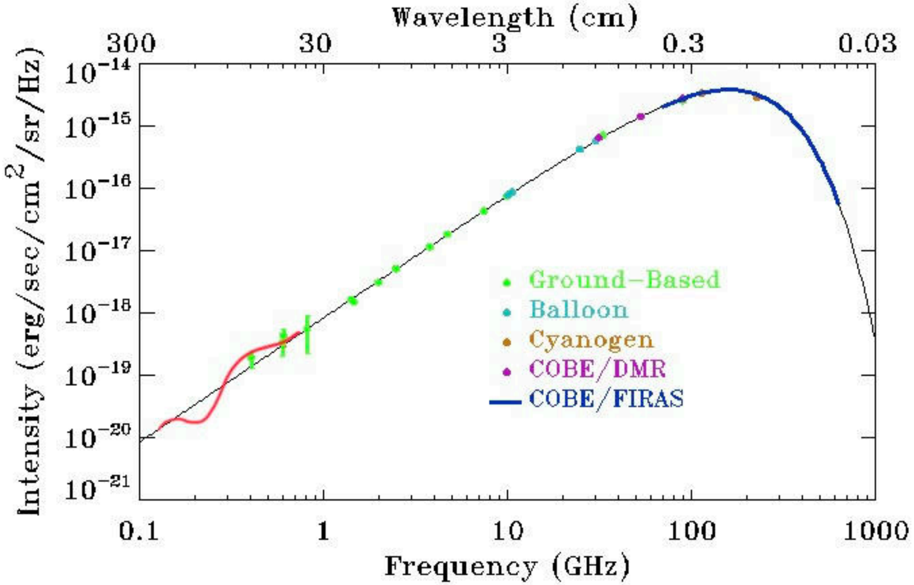

from [3]

The 21-cm signal

The *brigthtness temperature* describes the intensity of the 21-cm line

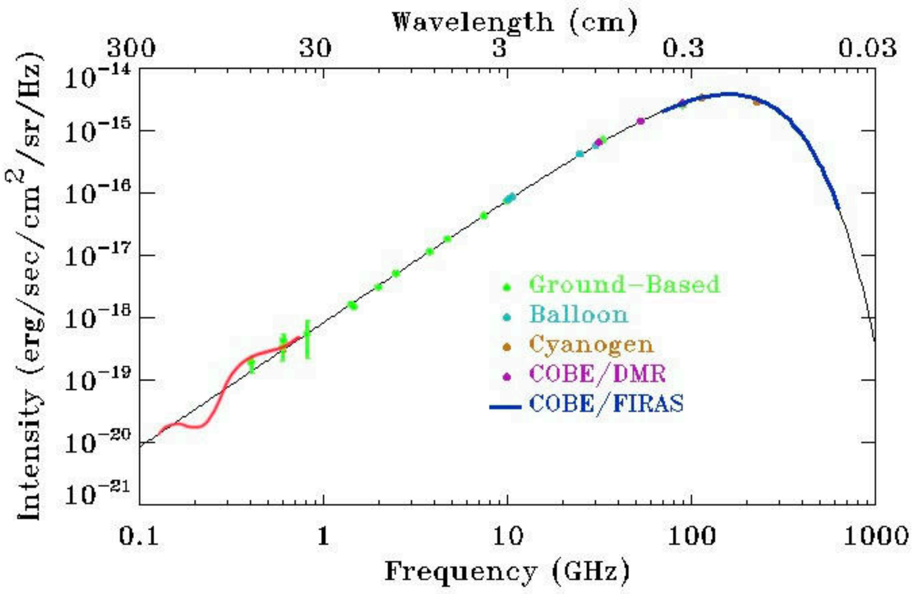

from [3]

remove contribution from the BB spectrum

differential brightness temperature

$\Longrightarrow$ the actual reionization signal

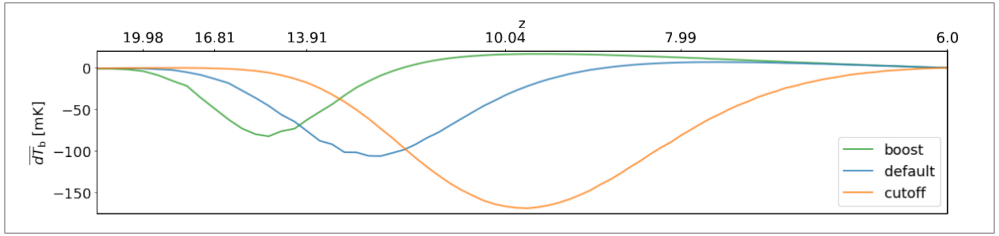

from [4]

Expression the 21-cm signal [1], [2]

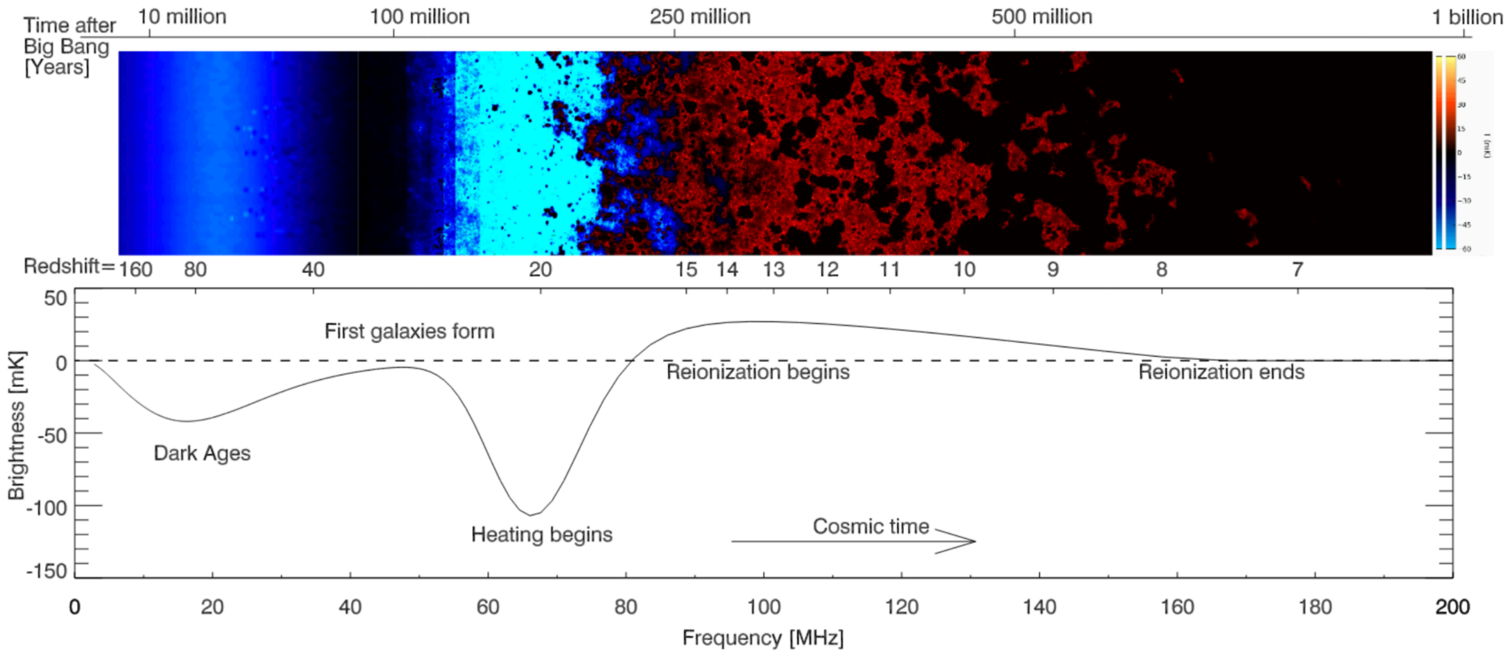

Expression the 21-cm signal [1], [2]

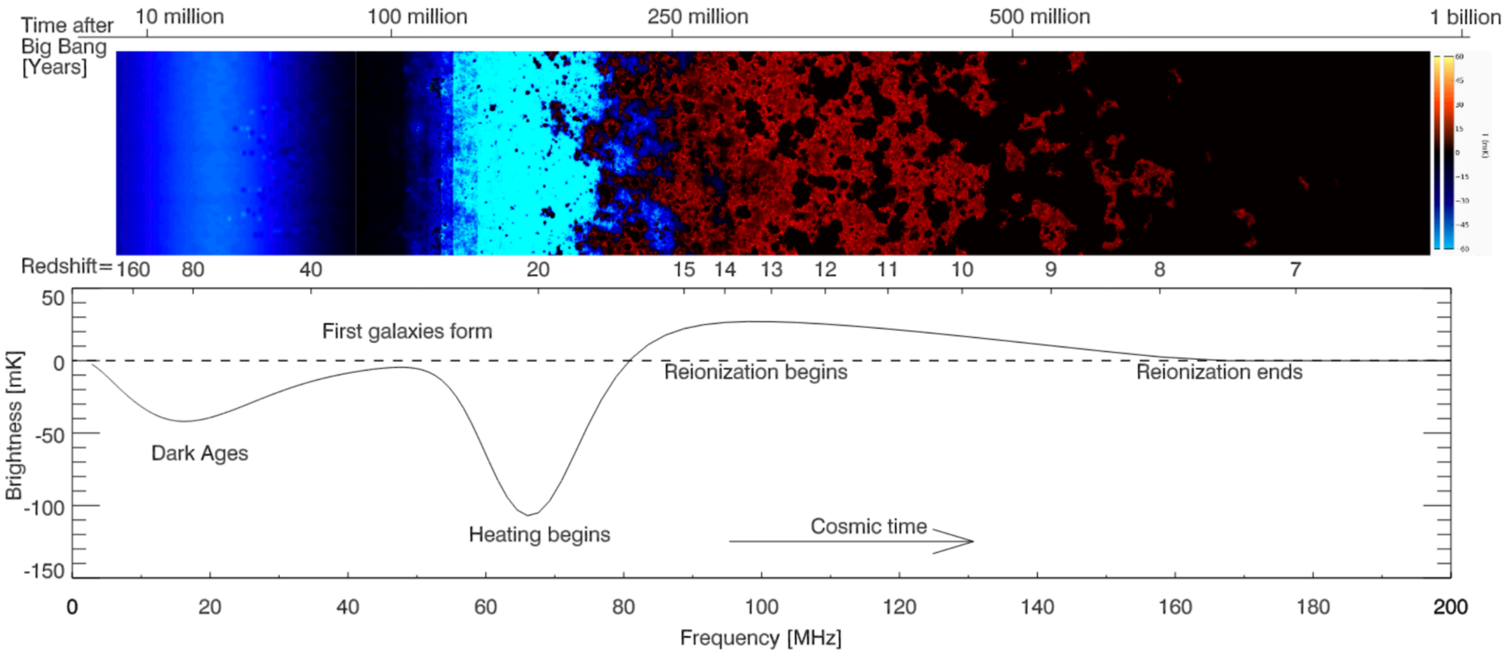

$$dT_{\mathrm{b}}(\boldsymbol{x}, z) \simeq T_0(z) \cdot \; x_{\mathrm{HI}}(\boldsymbol{x}, z) \; \cdot (1 + \delta_b(\boldsymbol{x}, z)) \cdot \frac{x_\alpha(\boldsymbol{x}, z)}{1 + x_\alpha(\boldsymbol{x}, z)} \cdot \left(\frac{1 - T_{\mathrm{CMB}}(z)}{T_{\mathrm{gas}}(\boldsymbol{x}, z)} \right)$$

The current state of simulations

Traditional approaches

$\rightarrow$ need to cover large dynamic range

$\rightarrow$ hydrodynamics & radiative transfer

$\rightarrow$ hard to scale

$\Rightarrow$ no reproducibility

The current state of simulations

Traditional approaches

→ need to cover large dynamic range

→ hydrodynamics & radiative transfer

→ hard to scale

⇒ no reproducibility

Semi-numerical approaches

such as `BEoRN` [4], `21cmFAST` [5]

→ approximative treatment

→ prediction of global signals

→ scalable + efficient

⇒ reproducible and flexible

BEoRN

- The halo model of reionization
- Revisiting the 21cm signal
- The “painting” procedure
- Postprocessing
- Maps
- Signal

Following [6], [7], the halo model describes (derivation):

The halo model of reionization

Following [6], [7], the halo model describes (derivation):

$$\rho_\alpha(r \mid M, z) = \frac{(1+z)^2}{4\pi r^2} \cdot \sum_{n=2}^{n_m} f_n \cdot \varepsilon_\alpha(\nu') \cdot f_\star \cdot \dot{M}(z' \mid M, z)$$

Following [6], [7], the halo model describes (derivation):

$$\rho_\alpha(r \mid M, z) = \frac{(1+z)^2}{4\pi r^2} \cdot \sum_{n=2}^{n_m} f_n \cdot \varepsilon_\alpha(\nu') \cdot f_\star \cdot \dot{M}(z' \mid M, z)$$

$$\frac{3}{2} \cdot \frac{\mathrm{d}\rho_h(r \mid M, z)}{\mathrm{d}z} = \frac{3\rho_h(r \mid M, z)}{1+z} - \frac{\rho_{\mathrm{xray}}(r \mid M, z)}{k_B(1+z)H(z)}$$

The halo model of reionization

Following [6], [7], the halo model describes (derivation):

$$\rho_\alpha(r \mid M, z) = \frac{(1+z)^2}{4\pi r^2} \cdot \sum_{n=2}^{n_m} f_n \cdot \varepsilon_\alpha(\nu') \cdot f_\star \cdot \dot{M}(z' \mid M, z)$$

$$\frac{3}{2} \cdot \frac{\mathrm{d}\rho_h(r \mid M, z)}{\mathrm{d}z} = \frac{3\rho_h(r \mid M, z)}{1+z} - \frac{\rho_{\mathrm{xray}}(r \mid M, z)}{k_B(1+z)H(z)}$$

$$\frac{\mathrm{d}V_b}{\mathrm{d}t} = \frac{\dot{N}_{\mathrm{ion}(t)}}{\overline{n}_H^0} - \alpha_B \cdot \frac{C}{a^3} \cdot \overline{n}_H^0 \cdot V_b$$

Visually:

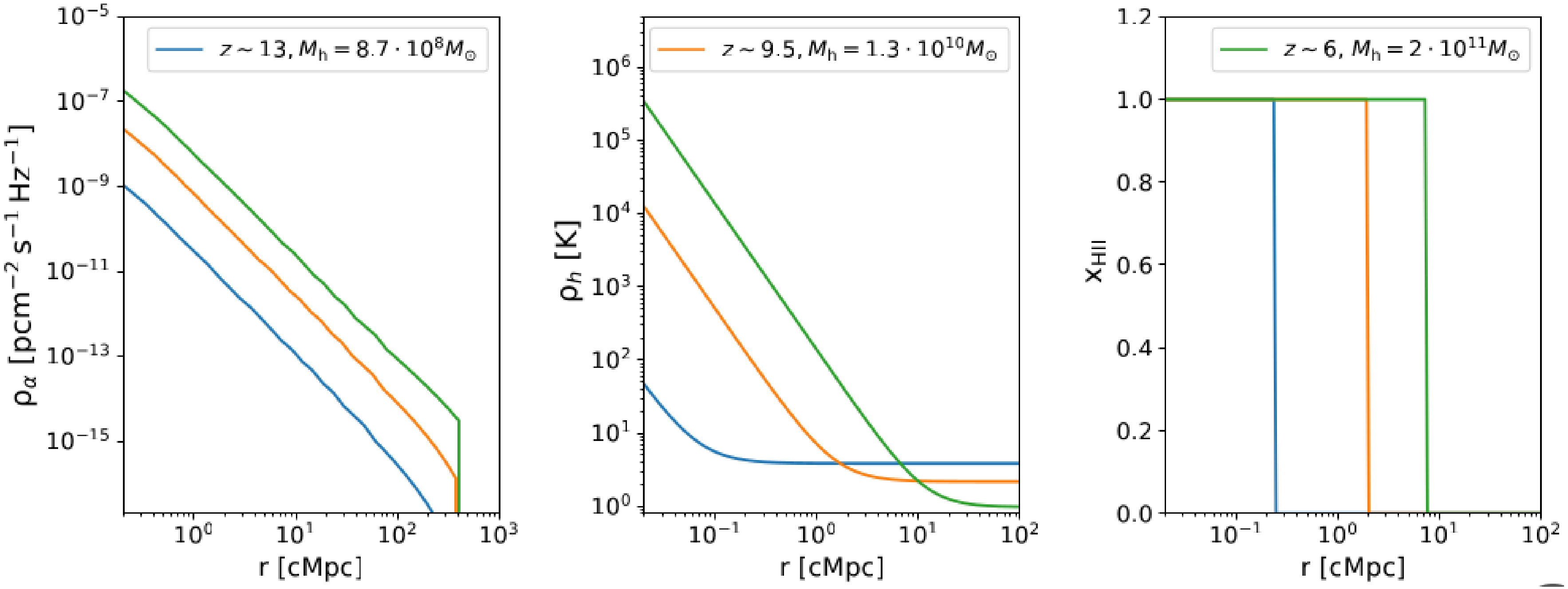

(from [4])

Revisiting the 21cm signal

$$dT_{\mathrm{b}}(\boldsymbol{x}, z) \simeq T_0(z) \cdot \; x_{\mathrm{HI}}(\boldsymbol{x}, z) \; \cdot (1 + \delta_b(\boldsymbol{x}, z)) \cdot \frac{x_\alpha(\boldsymbol{x}, z)}{1 + x_\alpha(\boldsymbol{x}, z)} \cdot \left(\frac{1 - T_{\mathrm{CMB}}(z)}{T_{\mathrm{gas}}(\boldsymbol{x}, z)} \right)$$

Revisiting the 21cm signal

$$dT_{\mathrm{b}}(\boldsymbol{x}, z) \simeq T_0(z) \cdot \ x_{\mathrm{HI}}(\boldsymbol{x}, z) \ \cdot (1 + \delta_b(\boldsymbol{x}, z)) \cdot \frac{x_\alpha(\boldsymbol{x}, z)}{1 + x_\alpha(\boldsymbol{x}, z)} \cdot \left(\frac{1 - T_{\mathrm{CMB}}(z)}{T_{\mathrm{gas}}(\boldsymbol{x}, z)} \right)$$

from x_{HII}

Revisiting the 21cm signal

$$dT_{\mathrm{b}}(\boldsymbol{x}, z) \simeq T_0(z) \cdot \; x_{\mathrm{HI}}(\boldsymbol{x}, z) \; \cdot (1 + \delta_b(\boldsymbol{x}, z)) \cdot \frac{x_\alpha(\boldsymbol{x}, z)}{1 + x_\alpha(\boldsymbol{x}, z)} \cdot \left(\frac{1 - T_{\mathrm{CMB}}(z)}{T_{\mathrm{gas}}(\boldsymbol{x}, z)} \right)$$

from x_{HII}

from ρ_α

Revisiting the 21cm signal

$$dT_\mathrm{b}(\boldsymbol{x}, z) \simeq T_0(z) \cdot \; x_\mathrm{HI}(\boldsymbol{x}, z) \; \cdot (1 + \delta_b(\boldsymbol{x}, z)) \cdot \frac{x_\alpha(\boldsymbol{x}, z)}{1 + x_\alpha(\boldsymbol{x}, z)} \cdot \left(\frac{1 - T_\mathrm{CMB}(z)}{T_\mathrm{gas}(\boldsymbol{x}, z)} \right)$$

from x_HII

from ρ_α

from ρ_h

The "painting" procedure

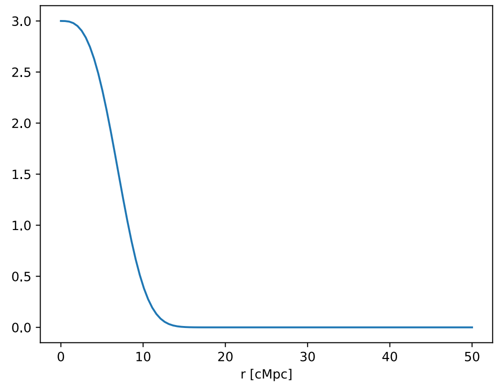

1-d profile

⟹

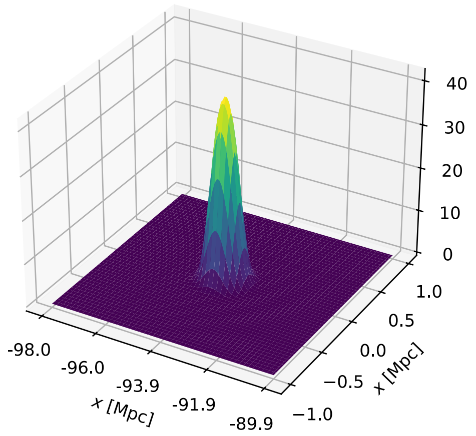

3-d kernel

(localized)

⟹

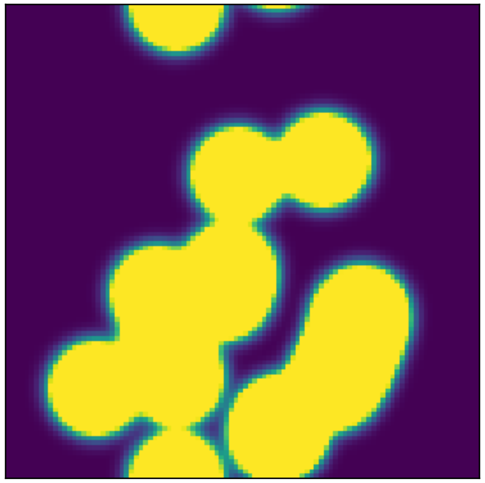

3-d contribution on a grid

The “painting” procedure

spherical symmetry

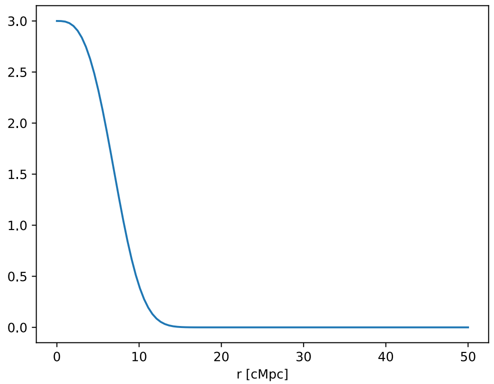

⟹

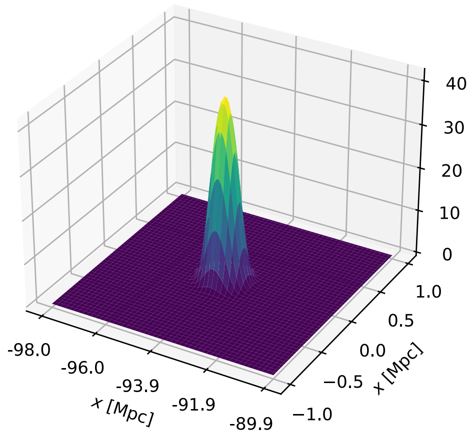

⟹

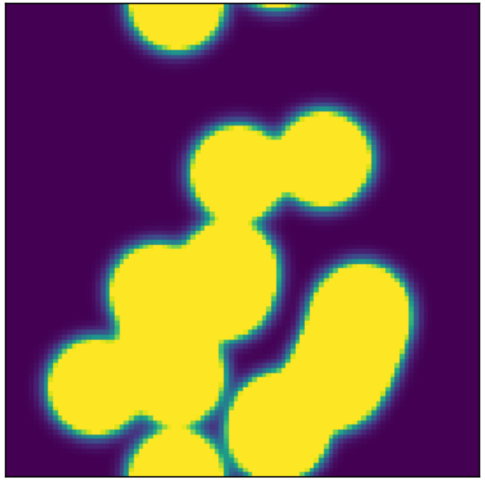

1-d profile

3-d kernel

(localized)

3-d contribution on a grid

The “painting” procedure

spherical symmetry

convolution (FFT)

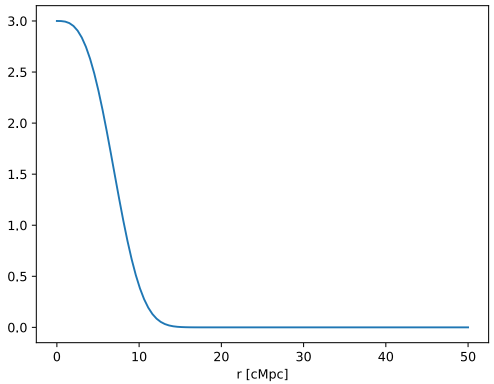

⟹

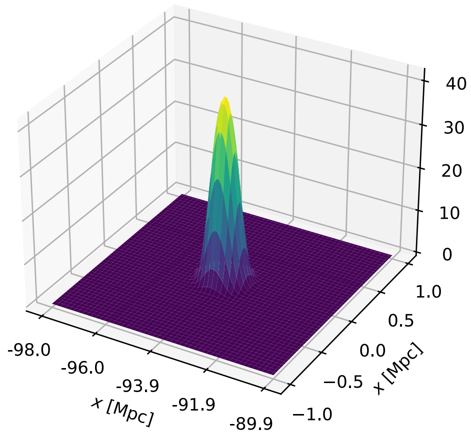

⟹

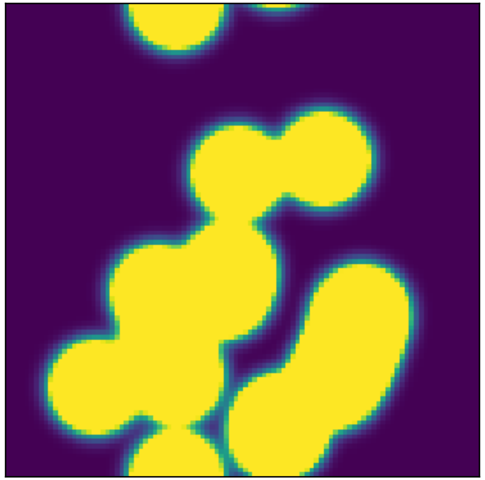

1-d profile

3-d kernel

(localized)

3-d contribution on a grid

The "painting" procedure

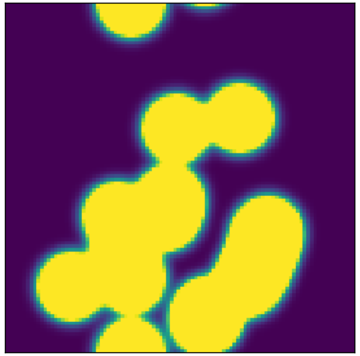

Multiple contributions $\Longrightarrow$

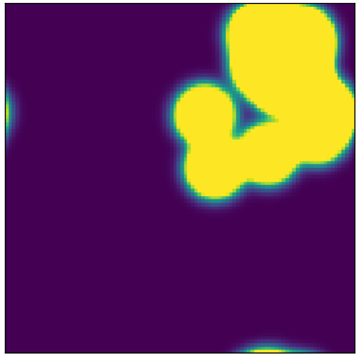

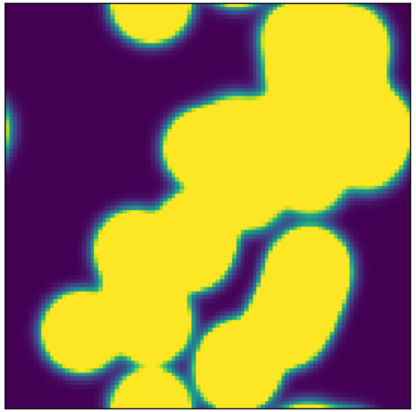

$\Longrightarrow$ *Postprocessing*

(overlaps, normalization, ...)

- ionization overlaps
- corrections due to RSD
- computation of derived quantities
- summary statistics

Through the redshifting of photons, the brightness temperature across redshift slices will be measured in a frequency band

⇒ representation as a lightcone

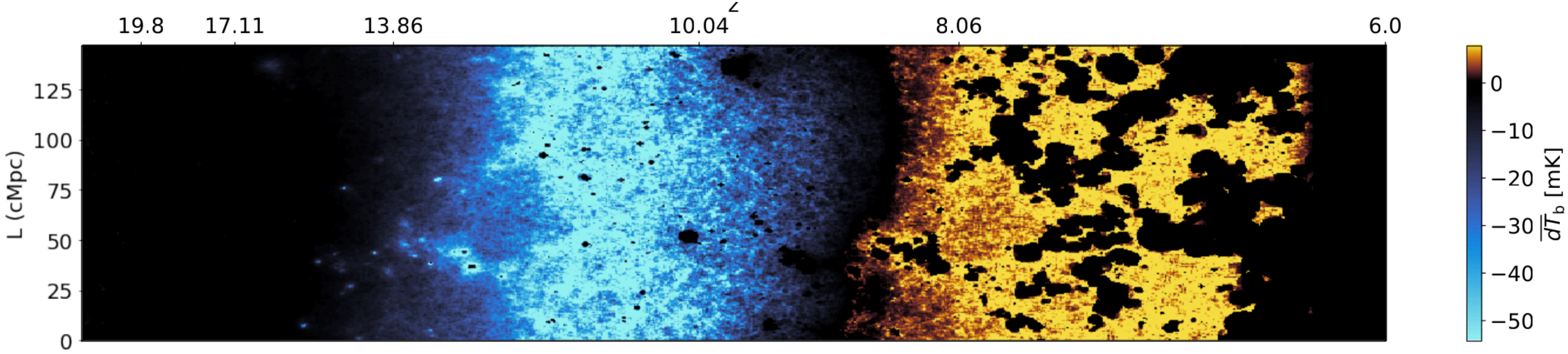

from [4]

Signal

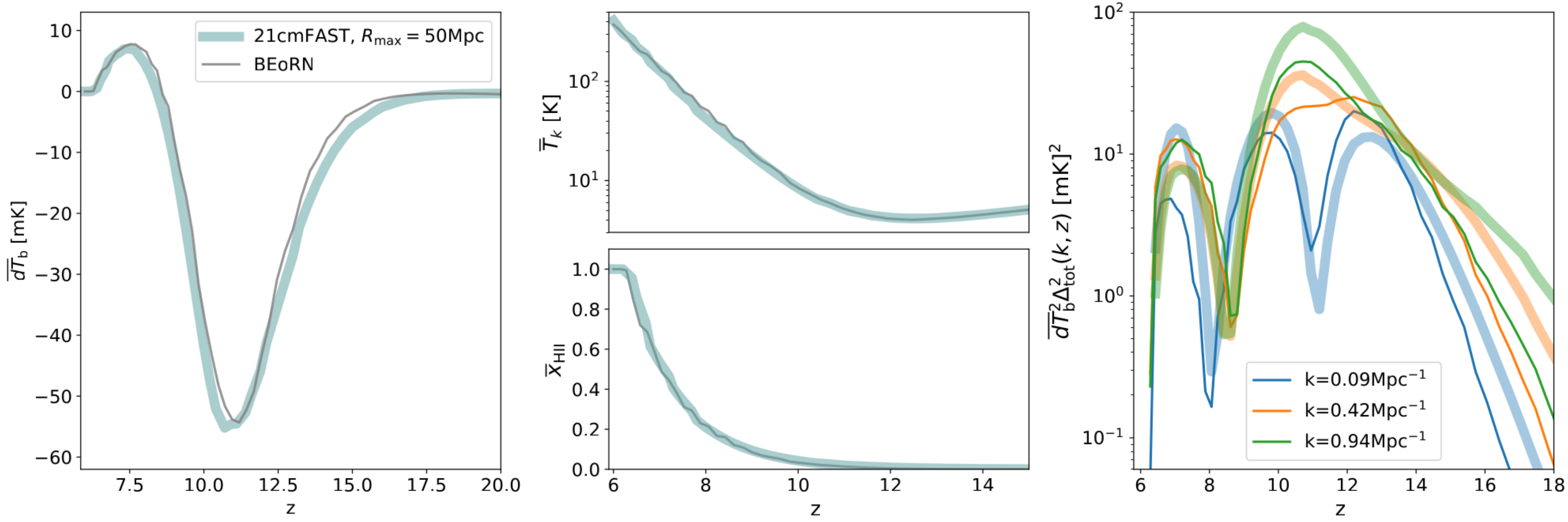

from [4]

Halo growth

- Motivation
- Effect on the flux profiles
- Inferring growth from THESAN data

Crucial dependence on the **star formation rate**

- assumed to be directly linked to halo growth rate $\dot{M}$:

$$\dot{M}_\star = f_\star(M_\mathrm{h}) \cdot \dot{M}_\mathrm{h}$$

- growth according to the exponential model:

$$M_\mathrm{h}(z) = M_\mathrm{h}(z_0) \cdot \exp[-\alpha(z - z_0)]$$

with $\alpha = \frac{\dot{M}_\mathrm{h}}{M_\mathrm{h}}$ the *specific growth rate*

Crucial dependence on the **star formation rate**

- assumed to be directly linked to halo growth rate $\dot{M}$:

$$\dot{M}_\star = f_\star(M_\mathrm{h}) \cdot \dot{M}_\mathrm{h}$$

- growth according to the exponential model:

$$M_\mathrm{h}(z) = M_\mathrm{h}(z_0) \cdot \exp[-\alpha(z - z_0)]$$

with $\alpha = \frac{\dot{M}_\mathrm{h}}{M_\mathrm{h}}$ the *specific growth rate*

→ inaccurate when applied to all halos

→ **inconsistent** with the N-body output

Crucial dependence on the **star formation rate**

- assumed to be directly linked to halo growth rate $\dot{M}$:

$$\dot{M}_\star = f_\star(M_\mathrm{h}) \cdot \dot{M}_\mathrm{h}$$

- growth according to the exponential model:

$$M_\mathrm{h}(z) = M_\mathrm{h}(z_0) \cdot \exp[-\alpha(z - z_0)]$$

with $\alpha = \frac{\dot{M}_\mathrm{h}}{M_\mathrm{h}}$ the *specific growth rate*

→ inaccurate when applied to all halos

→ **inconsistent** with the N-body output

→ how to implement **consistent** growth?

Effect on the flux profiles

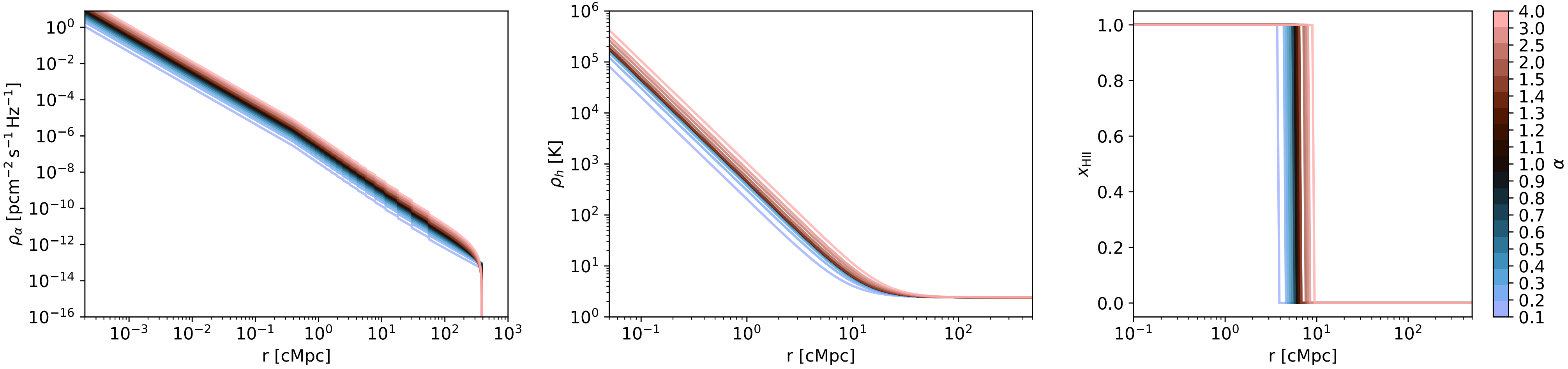

$M_{\rm h} = 6.08 \cdot 10^{11} M_\odot$ (fixed)

$\Longrightarrow$ correction up to $\times$ 5

Inferring growth from THESAN data

- already includes precomputed merger trees [8]
- follow main progenitor branch back in time
- fit the exponential model to main progrenitor branch
- use **individual growth** to select profile
- **self-consistent** treatment of halo growth leveraging the snapshots

Inferring growth from THESAN data

- already includes precomputed merger trees [8]
- follow main progenitor branch back in time
- fit the exponential model to main progrenitor branch
- use **individual growth** to select profile
- **self-consistent**∗ treatment of halo growth leveraging the snapshots

Inferring growth from Thesan data

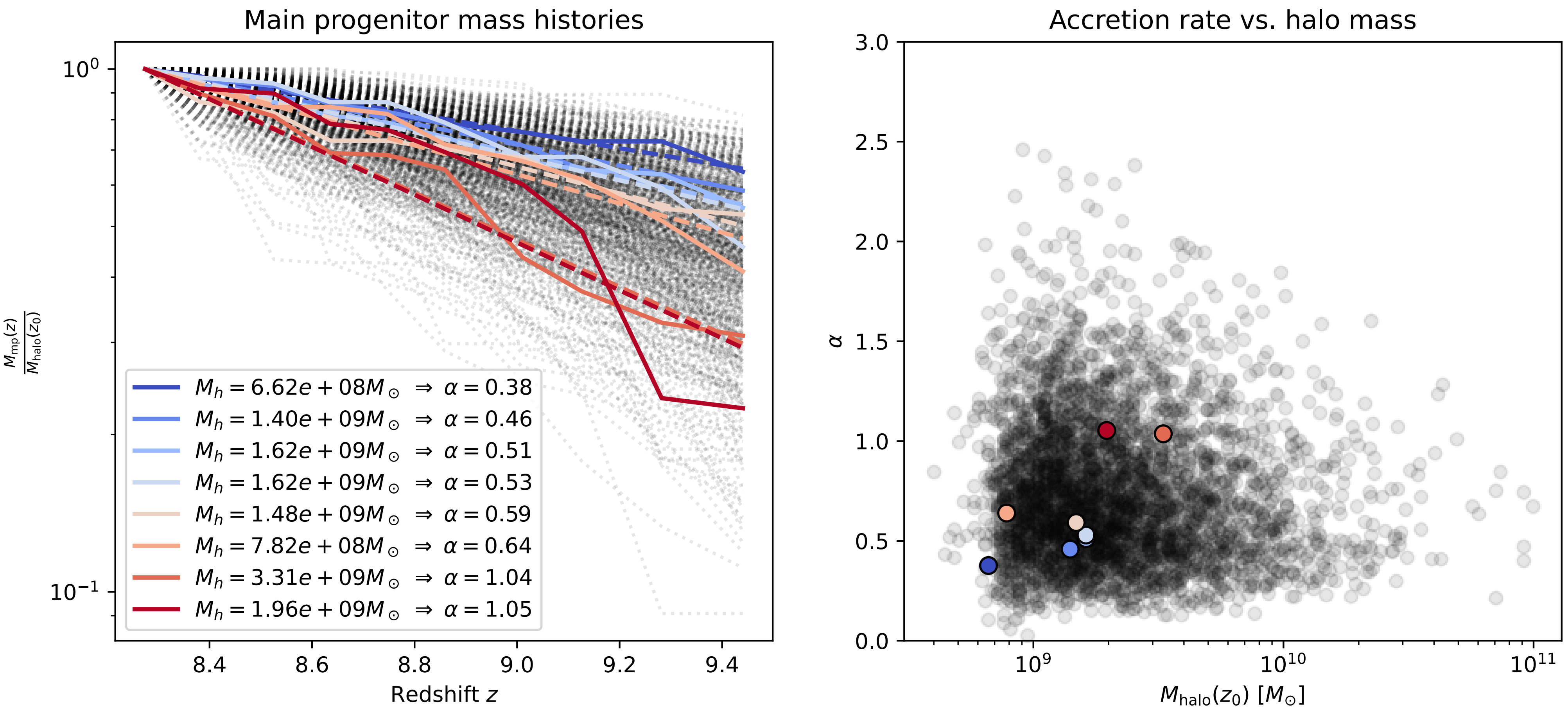

Adaptations

- Central changes
- Simplified usage

Central changes

- profile generation taking into account halo growth rate
- reading merger trees + inferring growth rates
- parallel painting across multiple halo bins
- performance and ease of use

Central changes

- profile generation taking into account halo growth rate
- reading merger trees + inferring growth rates
- parallel painting across multiple halo bins
- performance and ease of use

→ Validated ✅

Simplified usage

/beorn.py

```python
from pathlib import Path
import beorn


current_directory = Path(".")
## Setup the parameters
parameters_file = current_directory / "parameters.yaml"
parameters =
beorn.structs.Parameters.from_yaml(parameters_file)
# sample format:
# parameters.solver.redshifts = [6, 20]
# parameters.simulation.file_root = ... / "Thesan-Dark-1"

## Handling of the io
# this will interface with the input simulation
loader = beorn.load_input_data.ThesanLoader(
    parameters,
    is_high_res = True
)

cache_handler = beorn.io.Handler(current_directory /
"cache")
```

```python
output_handler = beorn.io.Handler(current_directory /
"output")
# handlers can also manage logs for us:
# output_handler.save_logs(parameters)


## Computation of the radiation profiles
solver =
beorn.radiation_profiles.ProfileSolver(parameters)
profiles = solver.solve()


## Full 3D painting of the radiation profiles over the
specified redshifts
painter = beorn.painting.Painter(
    parameters,
    loader = loader,
    cache_handler = cache_handler,
    output_handler = output_handler
)

grid = painter.paint_full(profiles)
# Done!
```

Results

— Map outputs
— Signals

Map outputs

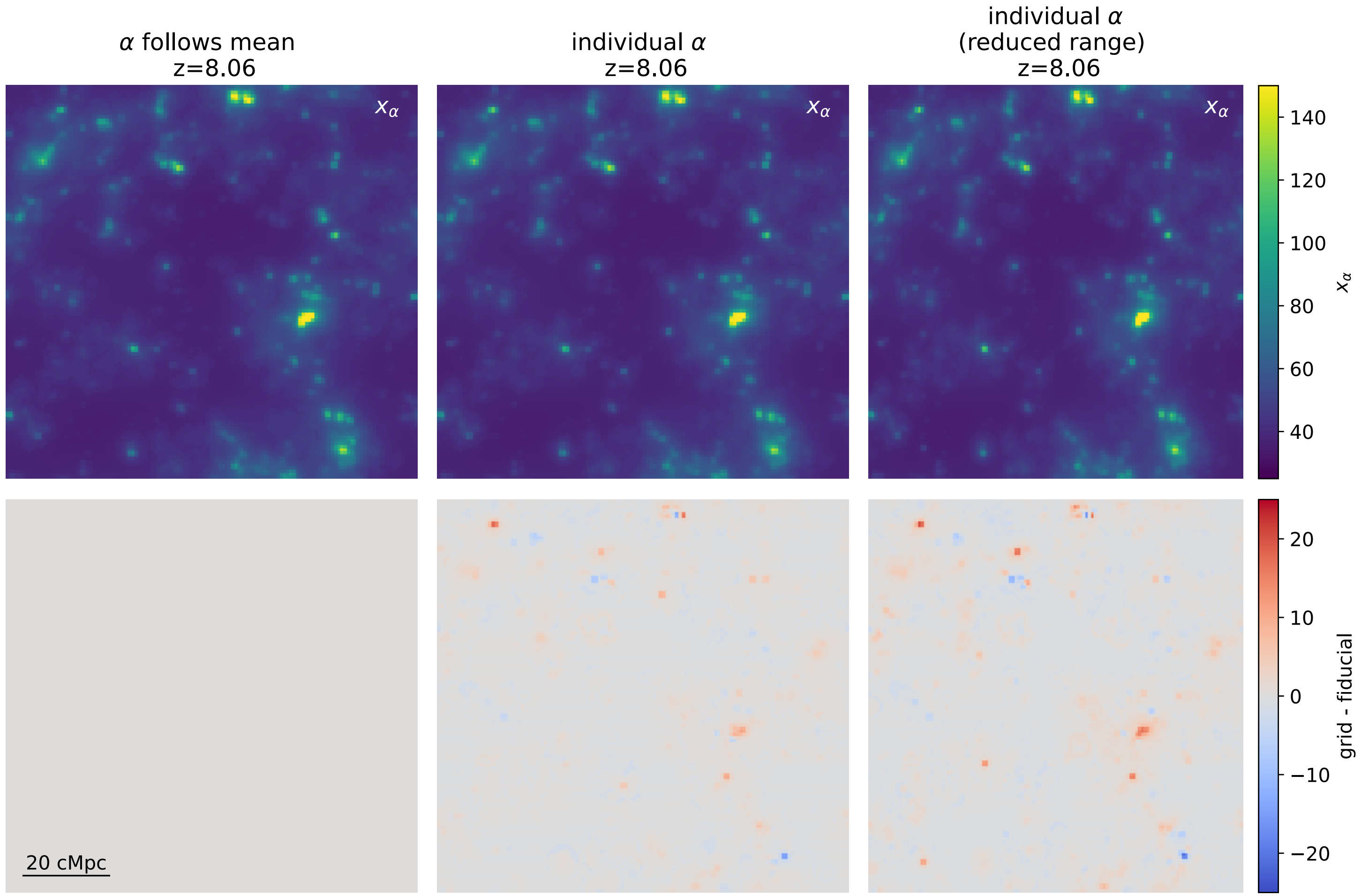

- strong variations close to sources
- nearly no effect in voids

Map outputs

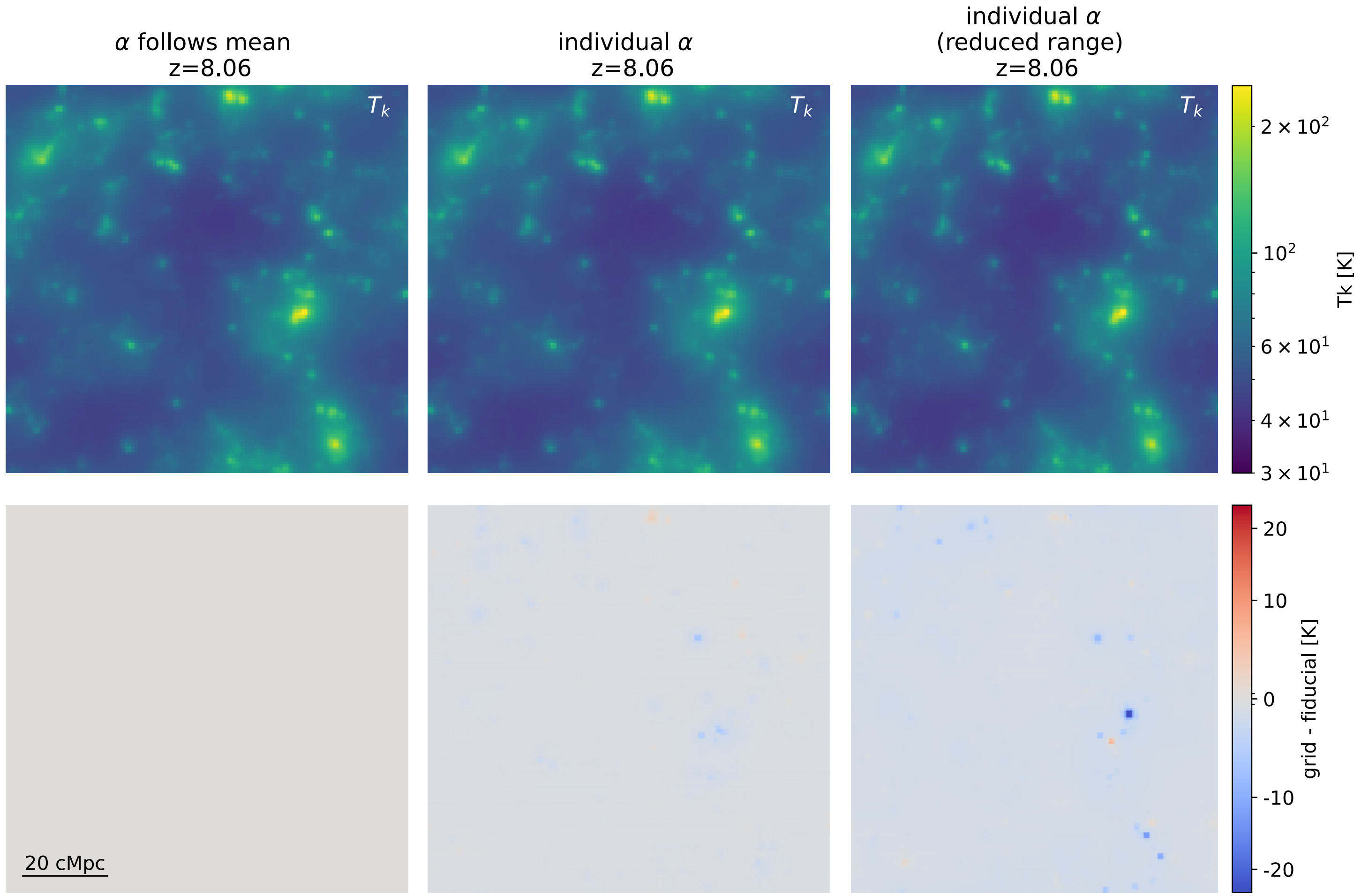

- delayed heating ⇔ colder halos
- highest accreting halos catch up

Map outputs

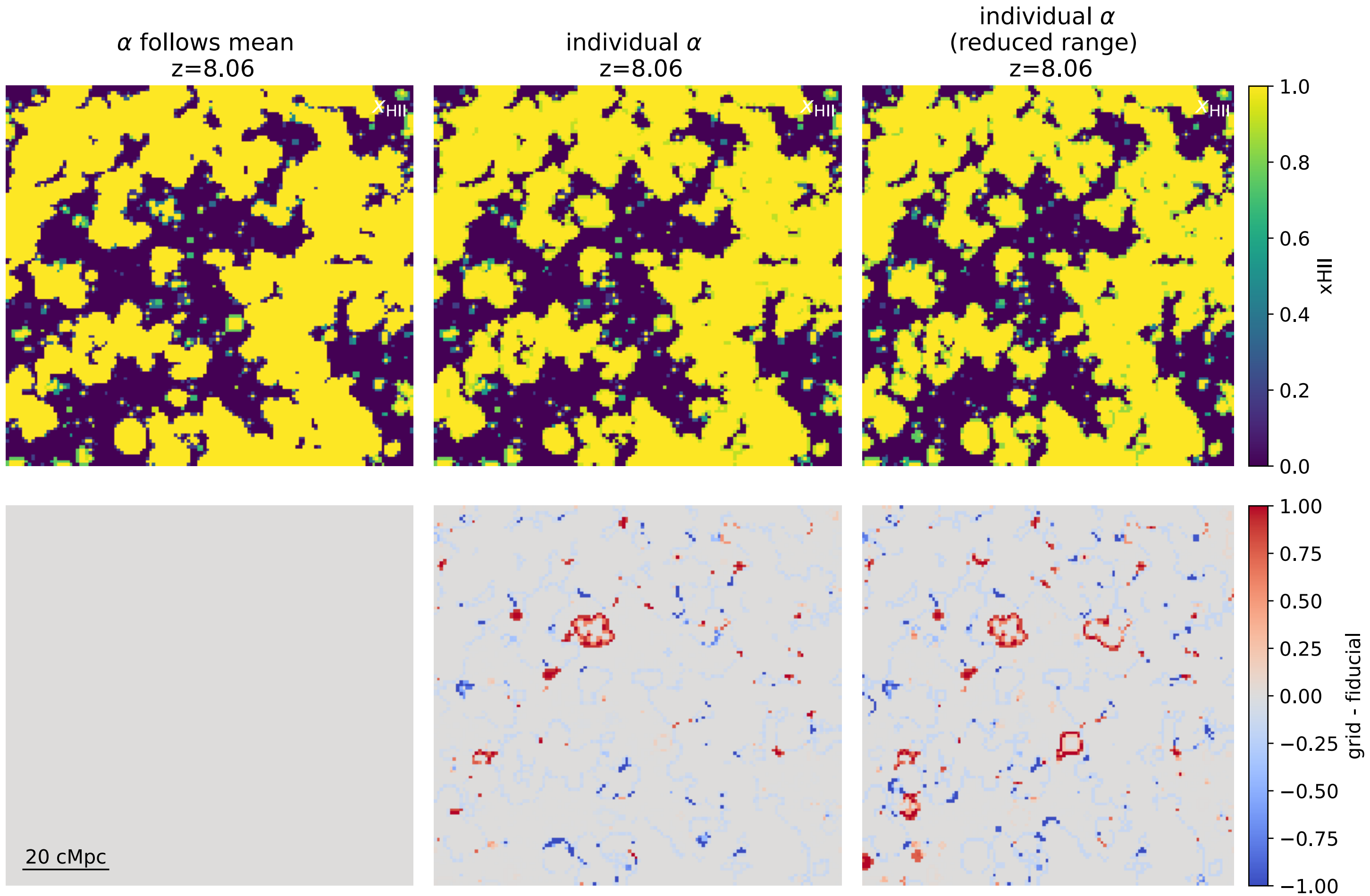

- high contrast due to sharp cutoffs
- clearly increased dynamic range

Map outputs

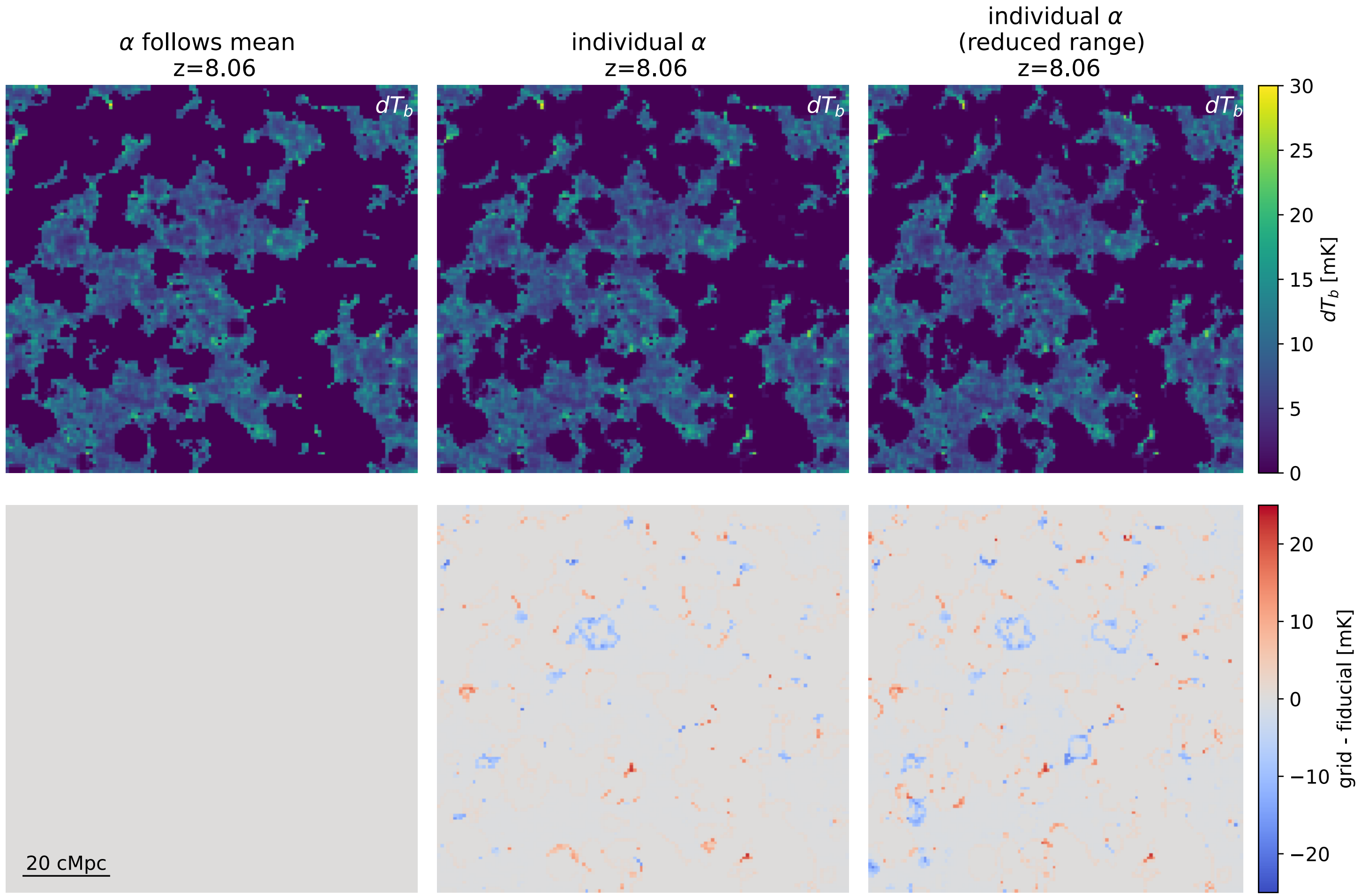

- richer structures due to combined effects
- clear distinction between "foreground" and "background" effects

Signals

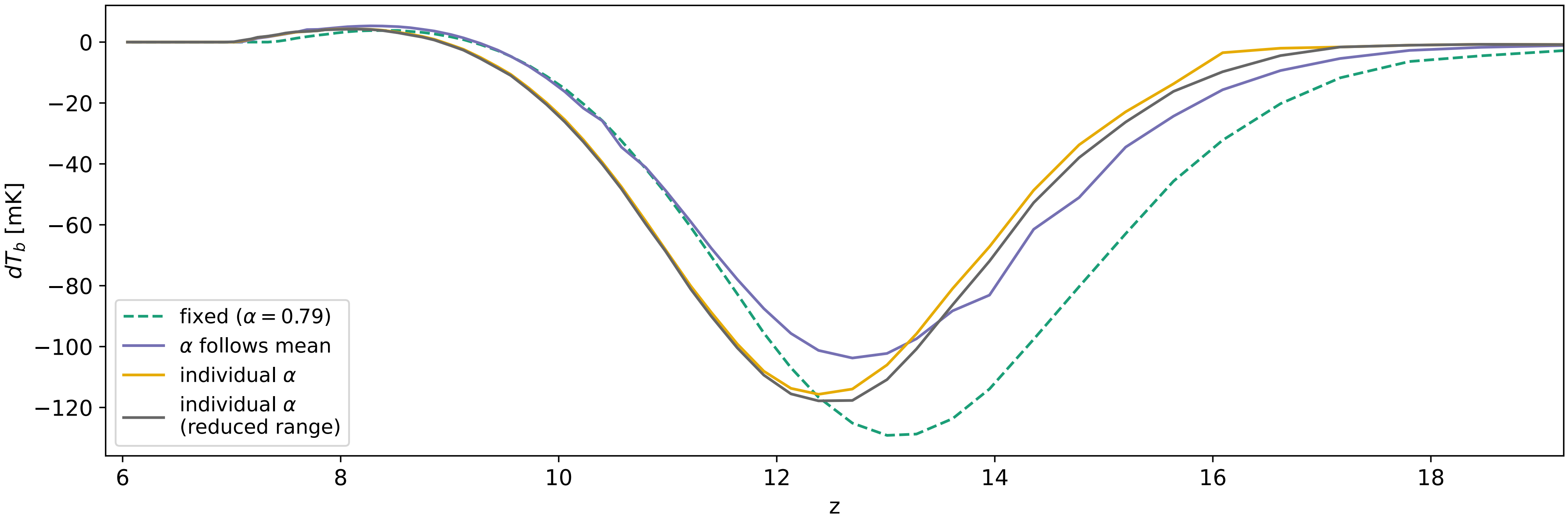

0
−20
−40
−60
−80
−100
−120
dT_b [mK]
6
8
10
12
14
16
18
z
fixed ($\alpha = 0.79$)
α follows mean
individual α
individual α
(reduced range)

Signals

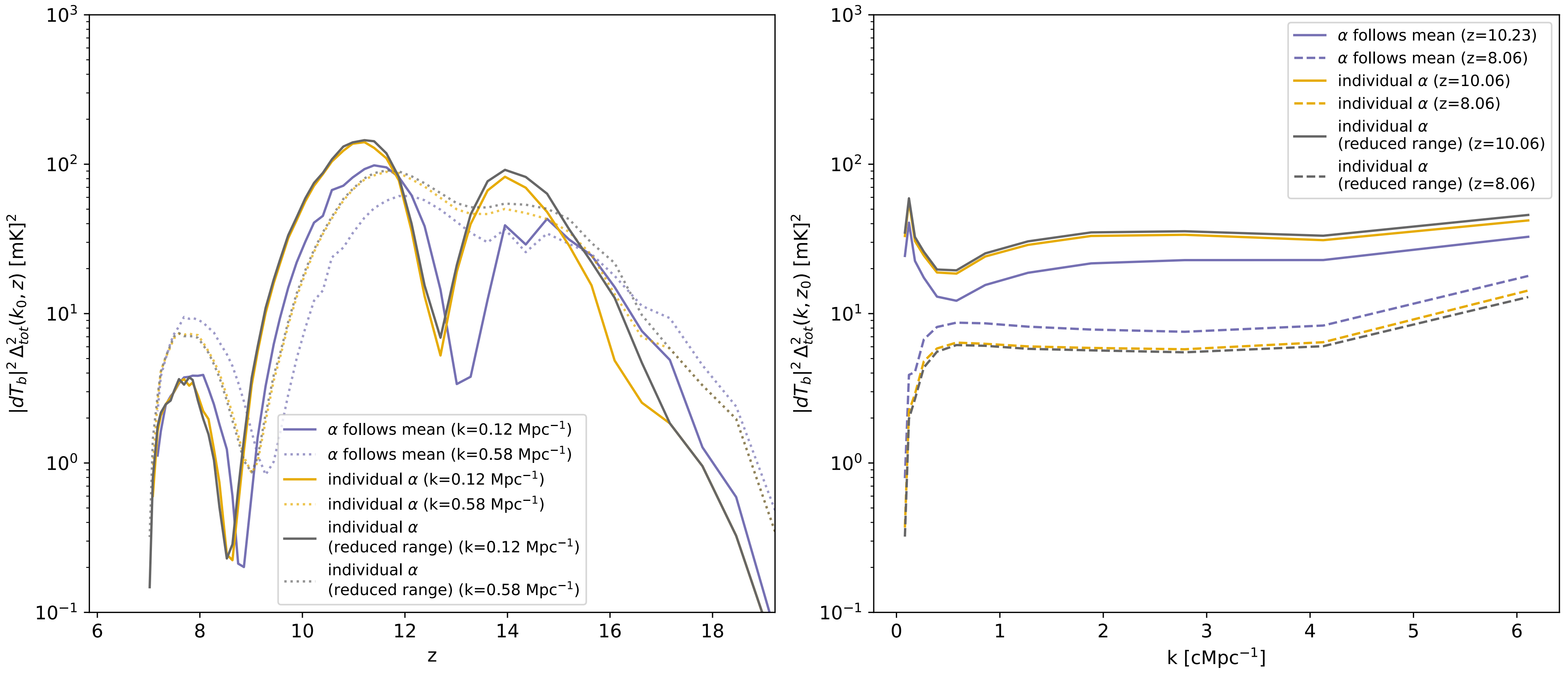

10^3
10^2
10^1
10^0
10^{-1}
$|dT_b|^2\,\Delta^2_{tot}(k_0, z)$ [mK]^2
6
8
10
12
14
16
18
z
α follows mean (k=0.12 Mpc^{-1})
α follows mean (k=0.58 Mpc^{-1})
individual α (k=0.12 Mpc^{-1})
individual α (k=0.58 Mpc^{-1})
individual α (reduced range) (k=0.12 Mpc^{-1})
individual α (reduced range) (k=0.58 Mpc^{-1})
$|dT_b|^2\,\Delta^2_{tot}(k, z_0)$ [mK]^2
0
1
2
3
4
5
6
k [cMpc^{-1}]
α follows mean (z=10.23)
α follows mean (z=8.06)
individual α (z=10.06)
individual α (z=8.06)
individual α (reduced range) (z=10.06)
individual α (reduced range) (z=8.06)

Conclusion

- Summary
- Outlook

Summary

- BEoRN a semi-numerical tool to simulate the 21-cm signal
  - uses the *halo model of reionization*
  - describes sources in terms of their host DM halo
  - $\Rightarrow$ central dependence on halo growth
- more accurate treatment of **individual** mass accretion
  - leads to significant changes to reionization history
  - map-level fluctuations
- BEoRN python package: https://github.com/cosmic-reionization/beorn
  - simulation-agnostic
  - easier to use
  - fully parallelized

Outlook

- further validation
- investigation + parameterization of stochasticity
- application to larger volumes

End

— Thank you for your attention

References

[1] J. R. Pritchard and A. Loeb, “21 cm cosmology in the 21st century,” *Reports on Progress in Physics*, vol. 75, no. 8, p. 86901, Aug. 2012, doi: 10.1088/0034-4885/75/8/086901.

[2] S. R. Furlanetto, S. Peng Oh, and F. H. Briggs, “Cosmology at low frequencies: The 21cm transition and the high-redshift Universe,” *Physics Reports*, vol. 433, no. 4–6, pp. 181–301, Oct. 2006, doi: 10.1016/j.physrep.2006.08.002.

[3] “CMB spectrum.” [Online]. Available: https://asd.gsfc.nasa.gov/archive/arcade/cmb_intensity.html

[4] T. Schaeffer, S. K. Giri, and A. Schneider, “<scp>beorn</scp>: a fast and flexible framework to simulate the epoch of reionization and cosmic dawn,” *Monthly Notices of the Royal Astronomical Society*, vol. 526, no. 2, pp. 2942–2959, Sep. 2023, doi: 10.1093/mnras/stad2937.

[5] A. Mesinger, S. Furlanetto, and R. Cen, “21cmfast: a fast, seminumerical simulation of the high-redshift 21-cm signal,” *Monthly Notices of the Royal Astronomical Society*, vol. 411, no. 2, pp. 955–972, 2011, doi: 10.1111/j.1365-2966.2010.17731.x.

[6] A. Schneider, S. K. Giri, and J. Mirocha, “Halo model approach for the 21-cm power spectrum at cosmic dawn,” *Physical Review D*, vol. 103, no. 8, Apr. 2021, doi: 10.1103/physrevd.103.083025.

[7] A. Schneider, T. Schaeffer, and S. K. Giri, “Cosmological forecast of the 21-cm power spectrum using the halo model of reionization.” [Online]. Available: https://arxiv.org/abs/2302.06626

[8] V. Springel *et al.*, “Simulations of the formation, evolution and clustering of galaxies and quasars,” *Nature*, vol. 435, no. 7042, pp. 629–636, Jun. 2005, doi: 10.1038/nature03597.

Full profiles

$$\rho_\alpha(r \mid M, z) = \frac{(1+z)^2}{4\pi r^2} \cdot \sum_{n=2}^{n_m} f_n \cdot \varepsilon_\alpha(\nu') \cdot f_\star \cdot \dot{M}(z' \mid M, z)$$

with the lookback redshift z' so $\nu' = \nu \cdot (1+z')/(1+z)$

$\Rightarrow$ coupling coefficient

$$x_\alpha(r \mid M, z) = \frac{1.81 \cdot 10^{11}}{1+z} \cdot S_\alpha(z) \cdot \rho_\alpha(r \mid M, z)$$

with a suppression factor $S_\alpha(z)$

Full profiles

$$\rho_{\mathrm{xray}}(r \mid M, z) = \frac{1}{r^2} \sum_i f_i f_{X,h} \cdot \int_{\nu_{\mathrm{th}}^i}^{\infty} d\nu \left(\nu - \nu_{\mathrm{th}}^i\right) h_P \sigma_i(\nu) e^{-\tau_\nu} f_\star \dot{M}(z' \mid M, z)$$

$$\Longrightarrow \frac{3}{2} \cdot \frac{\mathrm{d}\rho_h(r \mid M, z)}{\mathrm{d}z} = \frac{3\rho_h(r \mid M, z)}{1+z} - \frac{\rho_{\mathrm{xray}}(r \mid M, z)}{k_B(1+z)H(z)}$$

with the Boltzmann constant k_B and $H(z)$ is the Hubble parameter

Full profiles

The comoving ionized volume around a source of ionizing photons satisfies the differential equation

$$\frac{\mathrm{d}V}{\mathrm{d}t} = \frac{\dot{N}_{\mathrm{ion}(t)}}{\overline{n}_H^0} - \alpha_B \cdot \frac{C}{a^3} \cdot \overline{n}_H^0 \cdot V$$

bubble radius $R_b = \sqrt[3]{\frac{3}{4\pi} V(M, z)}$ and using the Heaviside step function θ_H:

$$x_{\mathrm{HII}}(r \mid M, z) = \theta_{\mathrm{H}}\left[R_b(M, z) - r\right]$$

Validation

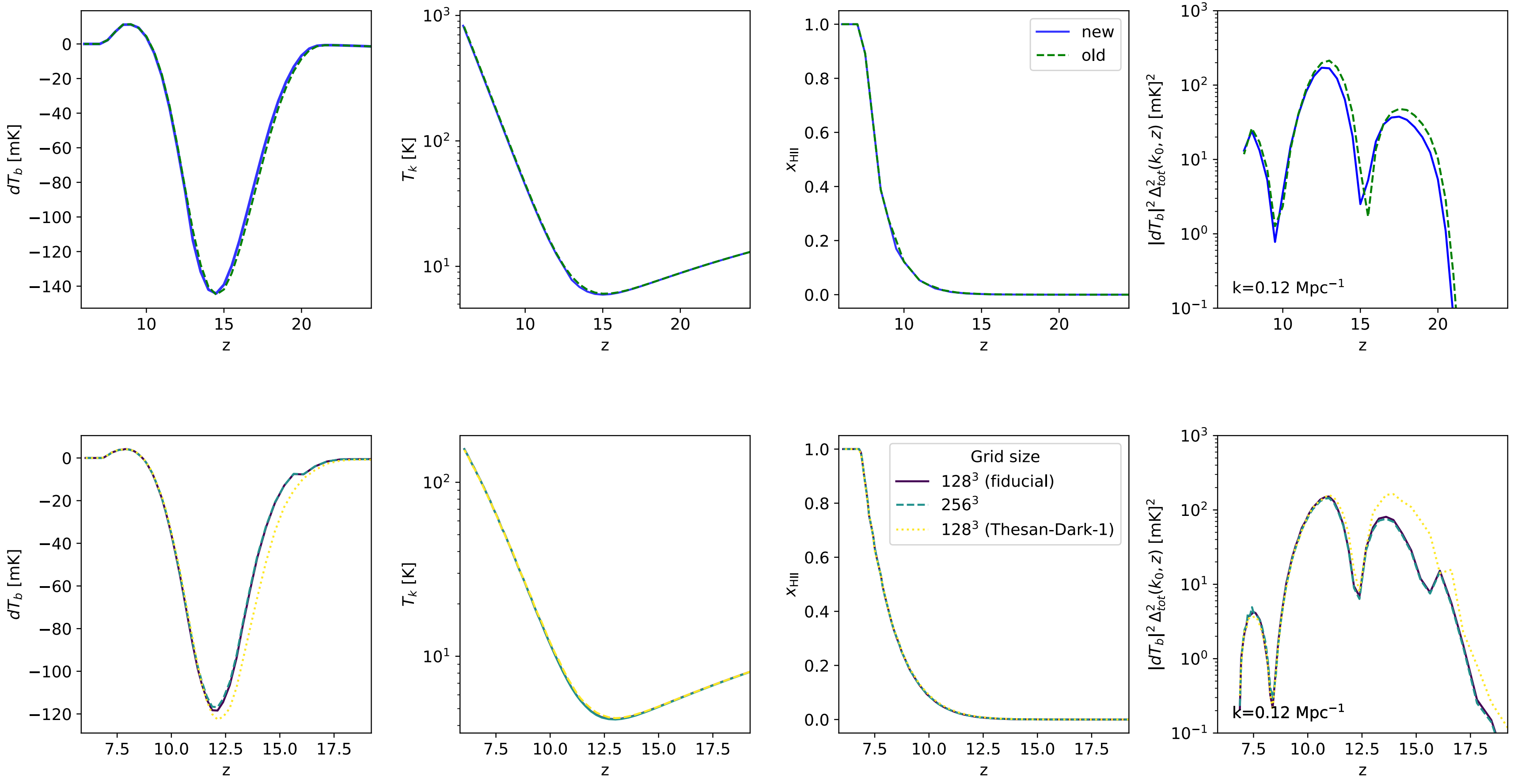
new
old
k=0.12 Mpc^{-1}
Grid size
128^3 (fiducial)
256^3
128^3 (Thesan-Dark-1)
k=0.12 Mpc^{-1}
dT_b [mK]
T_k [K]
x_{HII}
$|dT_b|^2 \Delta^2_{tot}(k_0, z)$ [mK]^2
z

Thesan resolution issues